NASA/TM—2010-216339

Analysis of the STS–126 Flow Control Valve Structural-Acoustic Coupling Failure

Trevor M. Jones, Jeffrey M. Larko, and Mark E. McNelis
Glenn Research Center, Cleveland, Ohio

May 2010

NASA STI Program . . . in Profile

Since its founding, NASA has been dedicated to the advancement of aeronautics and space science. The NASA Scientific and Technical Information (STI) program plays a key part in helping NASA maintain this important role.

The NASA STI Program operates under the auspices of the Agency Chief Information Officer. It collects, organizes, provides for archiving, and disseminates NASA's STI. The NASA STI program provides access to the NASA Aeronautics and Space Database and its public interface, the NASA Technical Reports Server, thus providing one of the largest collections of aeronautical and space science STI in the world. Results are published in both non-NASA channels and by NASA in the NASA STI Report Series, which includes the following report types:

- TECHNICAL PUBLICATION. Reports of completed research or a major significant phase of research that present the results of NASA programs and include extensive data or theoretical analysis. Includes compilations of significant scientific and technical data and information deemed to be of continuing reference value. NASA counterpart of peer-reviewed formal professional papers but has less stringent limitations on manuscript length and extent of graphic presentations.

- TECHNICAL MEMORANDUM. Scientific and technical findings that are preliminary or of specialized interest, e.g., quick release reports, working papers, and bibliographies that contain minimal annotation. Does not contain extensive analysis.

- CONTRACTOR REPORT. Scientific and technical findings by NASA-sponsored contractors and grantees.

- CONFERENCE PUBLICATION. Collected papers from scientific and technical conferences, symposia, seminars, or other meetings sponsored or cosponsored by NASA.

- SPECIAL PUBLICATION. Scientific, technical, or historical information from NASA programs, projects, and missions, often concerned with subjects having substantial public interest.

- TECHNICAL TRANSLATION. English-language translations of foreign scientific and technical material pertinent to NASA's mission.

Specialized services also include creating custom thesauri, building customized databases, organizing and publishing research results.

For more information about the NASA STI program, see the following:

- Access the NASA STI program home page at *http://www.sti.nasa.gov*

- E-mail your question via the Internet to *help@ sti.nasa.gov*

- Fax your question to the NASA STI Help Desk at 443–757–5803

- Telephone the NASA STI Help Desk at 443–757–5802

- Write to:
  NASA Center for AeroSpace Information (CASI)
  7115 Standard Drive
  Hanover, MD 21076–1320

NASA/TM—2010-216339

Analysis of the STS–126 Flow Control Valve Structural-Acoustic Coupling Failure

Trevor M. Jones, Jeffrey M. Larko, and Mark E. McNelis
Glenn Research Center, Cleveland, Ohio

Prepared for the
Spacecraft and Launch Vehicle Dynamic Environments Workshop
sponsored by The Aerospace Corporation
El Segundo, California, June 9–11, 2009

National Aeronautics and
Space Administration

Glenn Research Center
Cleveland, Ohio 44135

May 2010

Acknowledgments

We would like to acknowledge our MSFC and industry counterparts in this FCV anomaly investigation: Clay Fulcher, MSFC, Jacobs Engineering—GH2 structural dynamic analysis; Bruce Laverde, MSFC, Jacobs Engineering—GH2 structural acoustic analysis; Matt Casiano, MSFC—GH2 CFD analysis; Jeff Rayburn, MSFC—stress analysis; and Paul Blelloch, ATA Engineering—NX I–DEAS 5, PressMap, and IMAT software consultation. We would also like to acknowledge our GRC counterparts: Dr. Michael J. Barrett, GRC, chief engineer; Carol A. Quinn, GRC, project manager; Dr. Dexter Johnson, GRC, task point of contact, discipline lead engineer; and Scott B. Cutlip, GRC, CAD modeling and analysis.

Level of Review: This material has been technically reviewed by technical management.

Available from

NASA Center for Aerospace Information
7115 Standard Drive
Hanover, MD 21076–1320

National Technical Information Service
5301 Shawnee Road
Alexandria, VA 22312

Available electronically at http://gltrs.grc.nasa.gov

Analysis of the STS–126 Flow Control Valve Structural-Acoustic Coupling Failure

Trevor M. Jones, Jeffrey M. Larko, and Mark E. McNelis
National Aeronautics and Space Administration
Glenn Research Center
Cleveland, Ohio 44135

Abstract

During the Space Transportation System mission STS–126, one of the main engine's flow control valves incurred an unexpected failure. A section of the valve broke off during liftoff. It is theorized that an acoustic mode of the flowing fuel, coupled with a structural mode of the valve, causing a high cycle fatigue failure. This report documents the analysis efforts conducted in an attempt to verify this theory. Hand calculations, computational fluid dynamics, and finite element methods are all implemented and analyses are performed using steady-state methods in addition to transient analysis methods. The conclusion of the analyses is that there is a critical acoustic mode that aligns with a structural mode of the valve.

Introduction

During the ascent phase of the Space Transportation System (STS) mission STS–126 an anomaly occurred. The gaseous hydrogen (GH2) flow control valve (FCV) of engine no. 2 of the main propulsion system appeared to switch from low towards a high flow position without being commanded to do so. Despite this anomaly the mission was successfully completed (Refs. 1 and 2).

Upon completion of the STS–126 flight the FCV was removed and inspected. The FCV poppet head was damaged; approximately one quarter of the poppet head circumference was broken-off as showing in Figure 1. Optical and scanning electron microscope (SEM) examination of the fracture surface was performed. The fracture surface exhibited distinct “thumbnail” and “bench mark” features that are indicative of a fatigue crack. The fracture surface contained several distinct zones that might indicate that several different events or load cases caused the propagation of the crack. No evidence was found that would indicate any raw material defect or flaw. The fracture surface did not indicate that hydrogen embrittlement was a significant contributor to the failure. The conclusion of this examination is that the failure was caused by high cycle fatigue (Refs. 1 and 2).

There are several important risks associated with this type of failure. If more than one FCV were to fail the orbiter External Tank (ET) might become over-pressurized. Another risk is internal damage to the Orbiter and ET hardware caused by the liberated FCV failure debris. If the liberated debris were to puncture a fuel line the result could be an explosion in the main engine compartment resulting in loss of vehicle. Another risk is under-pressurization of the ET due to blockage of the ET lines caused by the debris.

This is the first failure of this type on a STS mission. The hypothesis is that an acoustic environment frequency coupled with a structural mode of the poppet causing a high cycle fatigue failure. The NASA Marshall Space Flight Center (MSFC) was assigned to perform acoustic and computational fluid dynamic (CFD) analysis as well as GH2 modal analysis in an effort to validate this hypothesis. The NASA Glenn Research Center (GRC) was tasked with verifying the structural dynamic and acoustic modeling and analysis of the GH2 flow control valve. GRC was to perform a similar analysis to MSFC using independent tools and methods to ensure the validity of the results. This report documents the work done by GRC in order to validate the work being done by MSFC.

Background

The Main Propulsion System (MPS) of the space shuttle consists of three main engines mounted on the rear of the orbiter. The engines are fueled with liquid hydrogen and liquid oxygen that is stored in the ET. The fuel is partially burned in a pre-chamber to produce hot gases at high pressure. The gas is then burned in the main combustion chamber and forced through the nozzles (see Fig. 2 for an engine schematic). The thrust rate can be controlled between approximately 65 to 109 percent thrust (Ref. 3).

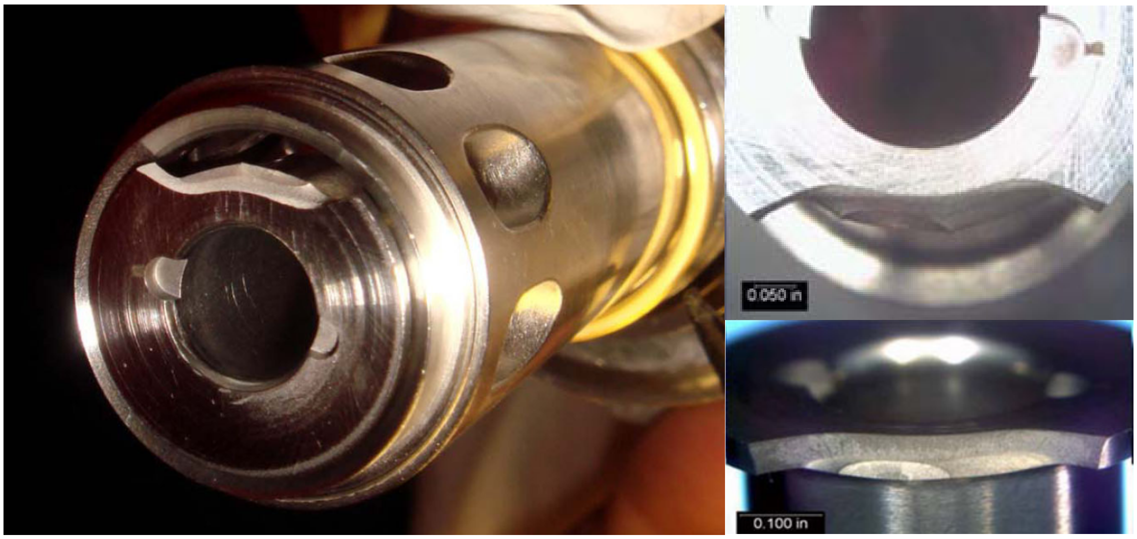

Figure 1.—STS–126 Damaged FCV Post Flight.

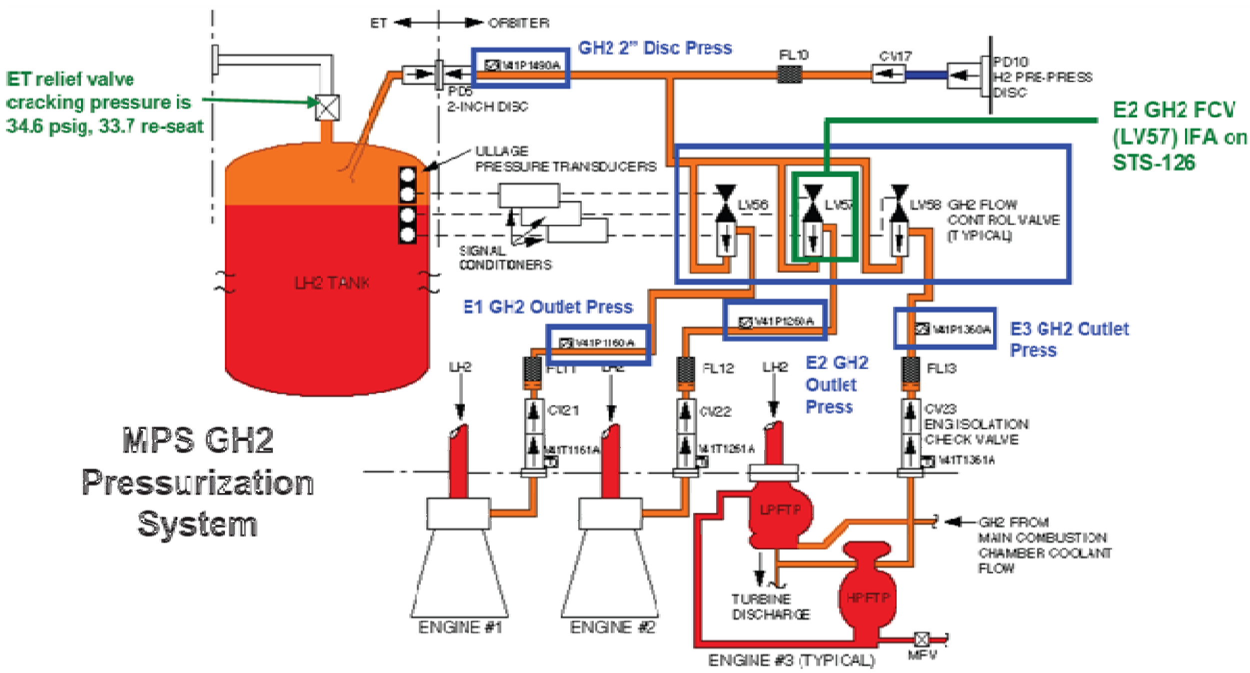

Figure 2.—Main Propulsion System Pressurization System Schematic.

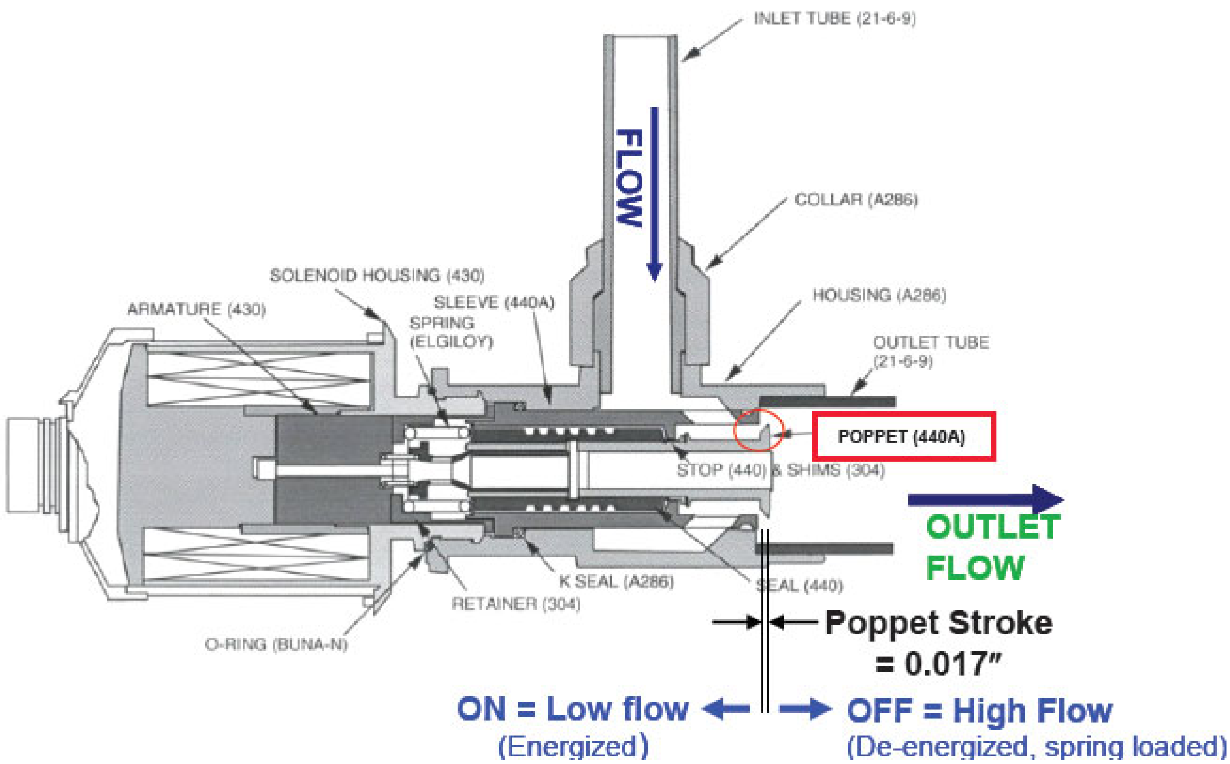

Figure 3.—Orbiter MPS GH2 Flow Control Valve Section View.

As part of the MPS, the FCV's regulate GH2 pressurant to the ET LH2 tank during ascent. There is one FCV for each of the three main engines. The poppet of the FCV is actuated by a spring-loaded solenoid. The solenoid is either on or off. When the solenoid is on, or energized, the valve is in a low flow state. In the low flow state gas is still flowing through the valve. The flow is restricted so a relatively high static pressure exists on the poppet flange. When the solenoid is off, or de-energized, the valve is in a high flow state; a relatively large quantity of gas is able to flow through the valve. The H2 gas flows from the engine through annuluses on the FCV housing around the poppet flange and back to the ET. Figure 3 shows a detailed schematic of the FCV assembly.

Critical Frequency Calculation

The first step taken in verifying the structural acoustic coupling is to determine the frequency range of interest using basic hand calculations. The critical frequency is the coupling frequency at which the acoustic mode most efficiently excites the structural response. The critical frequency is given by the following equation (Ref. 4):

$$f_c = \frac{c^2}{1.8 c_L t} \tag{1}$$

f_c	critical frequency
t	structure thickness
c_L	structural longitudinal bending wavespeed
c	speed of sound in a gaseous medium

The structural thickness is simply the width of the FCV poppet fracture surface. This value is a constant. The structural longitudinal bending wavespeed is a function of the geometry and material properties. This value will remain constant. The structural longitudinal bending wavespeed is given by the following equation (Ref. 4):

$$c_L = \sqrt{\frac{E}{\rho_m}} \tag{2}$$

E modulus of elasticity

ρ_m density

The speed of sound in a gaseous medium is a function of the density of the gas and is varied. The gaseous medium is GH2. The density of the GH2 is determined using CFD data provided by MSFC. This value varies depending on the flow condition; the density is different for the low verses the high flow configuration. The value varies depending on where the measurement is taken. The density of the GH2 gas is computed on both the inside (c_1) and immediately outside (c_2) of the poppet flange as shown in Figure 4.

This yields a total of four independent values for the speed of sound in the critical frequency calculation. The poppet material is 440 stainless steel and it is assumed to be homogeneous. The poppet flange is idealized as a beam in bending. Table 1 summarizes all of the input values and the resulting four values of critical frequency. Based on these results the frequency range of interest is approximately 94.9 to 128.5 kHz.

TABLE 1.—CRITICAL FREQUENCY RESULTS

High flow		
Variable	Value	Units
E	2.9×10^7	lbf/in.^{2}
ρ_m	0.276	lbf/in.^{3}
c_L	201,384	in./sec
t	0.075	in.
$c_{1\text{-high}}$	58,680	in./sec
$c_{2\text{-high}}$	51,645	in./sec
$f_{1\text{-high}}$	126,066	Hz
$f_{2\text{-high}}$	97,685	Hz

Low flow		
Variable	Value	Units
E	2.9×10^7	lbf/in.^{2}
ρ_m	0.276	lbf/in.^{3}
c_L	201,384	in./sec
t	0.075	in.
$c_{1\text{-high}}$	59,246	in./sec
$c_{2\text{-high}}$	50,914	in./sec
$f_{1\text{-high}}$	128,512	Hz
$f_{2\text{-high}}$	94,904	Hz

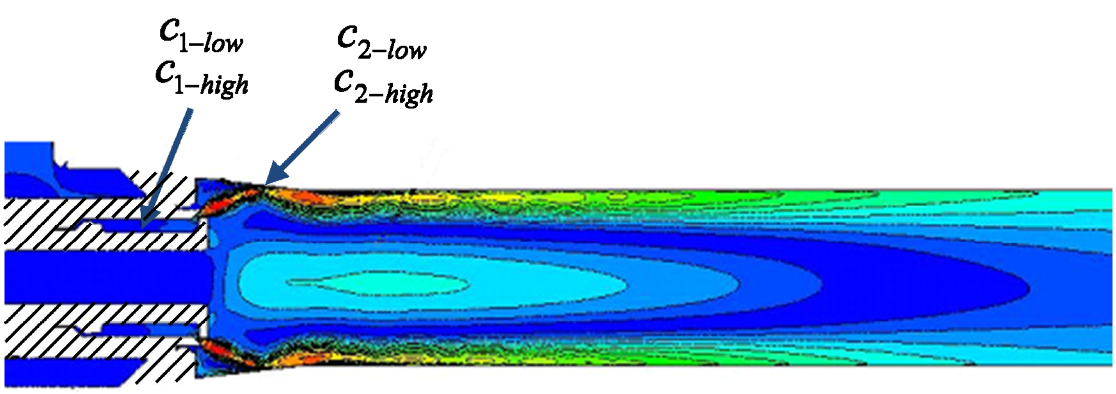

Figure 4.—FCV Poppet CFD Results and Measurement Locations.

Cavity Acoustic Modes

In order to determine the existence of structural acoustic coupling it is important to understand the acoustic modes of the FCV cavity. This section investigates the acoustic modes of the FCV cavity using a combination of tools and methods.

MSFC was primarily responsible for analyzing the acoustic modes of the FCV cavity. MSFC used several different methods to analyze the FCV cavity. Figure 4 is a graphical representation of MSFCs analysis results. The dashed lines running diagonal on the plot bound the bands where one would expect to find acoustic modes for the various families of acoustic mode type. These acoustic predictions were computed using a combination of hand calculations, MSC.Nastran, and Matlab. CFD solutions for the acoustic modes were also computed. High and low flow configurations at both 72 and 104.5 percent thrust were considered for both STS–119 and STS–126. This is a total of eight cases for the CFD analysis. The results for the eight cases are overlaid with the acoustic predictions on Figure 4. The relative size of the shapes indicates the relative energy levels present between the cases; a larger shape indicates a higher energy acoustic mode. The highest energy modes all seem to be clumped at 107.4 kHz. 107.4 kHz falls in the range for the critical frequency previously determined in the GRC hand calculations.

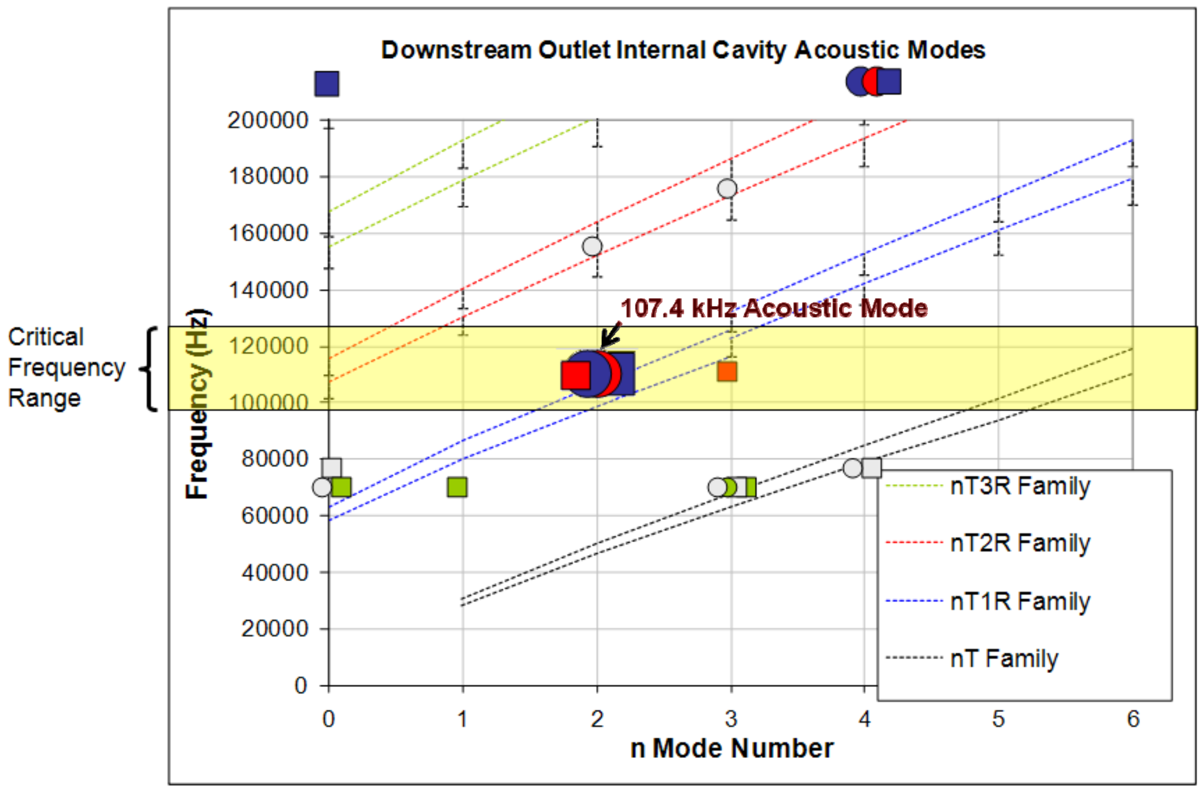

Thrust	STS 119 HF	STS 119 LF	STS 126 HF	STS 126 LF
104.5%	Case1	Case3	Case5	Case7
72%	Case2	Case4	Case6	Case8

Figure 4.—GH2 FCV Internal Cavity Acoustic Modes.

FCV Structural Modes

In order to determine the existence of structural acoustic coupling it is important to understand the structural modes of the poppet. This section investigates the structural modes of the poppet using both hand calculations based on tabulated idealized configurations as well as through the use of finite element (FE) methods.

The first attempt at understanding the structural modes of the poppet was done using idealized hand calculations. The purpose of this calculation is to roughly determine the frequency of the poppet first bending mode. This information is used to increase confidence in the results from the finite element model (FEM). For this calculation the poppet is being idealized as a constant section annulus tube clamped at one end and free at the other. The equation for the natural frequency of this structure is given by the following equation (Ref. 5):

$$f_i = \frac{\lambda_i^2}{2\pi L^2}\sqrt{\frac{EI}{m}} \tag{3}$$

$$I = \frac{\pi}{4}\left(a^4 - b^4\right) \tag{4}$$

f_i	natural frequency
λ_i	function of boundary condition
L	length of beam
E	modulus of elasticity
m	mass per unit length of beam
I	area moment of inertia about neutral axis

Annulus section

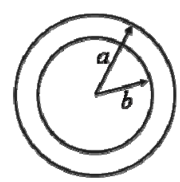

λ is a dimensionless parameter that is a function of our boundary condition; it is based on tabulated values. Only the first bending mode of the poppet is calculated here. The length of the beam is the distance from where the poppet is fixed, to the far face of the free end. The modulus of elasticity is the modulus of 440A stainless steel. The mass per unit length is the mass of the cantilevered portion of the beam divided by length of that portion. The area moment of inertia is based on the cross section dimensions of the poppet. Table 2 summarizes all the input values used and the resulting frequency for the poppet first bending mode.

TABLE 2.—NATURAL FREQUENCY RESULTS

Variable	Value	Units
λ_1	1.875	------
L	0.77	in.
E	2.9×10^{7}	lbf/in.^{2}
m	2.1×10^{-4}	lbf/g
I	2.29×10^{-3}	in.^{4}
a	0.24	in.
b	0.141	in.
f_1	16,795	Hz

This calculation yields the first bending mode of the poppet at around 17 kHz. 17 kHz is high compared to what one might expect the first mode of a structure or part to be because the poppet is small and light weight; the cantilevered portion of the poppet is only 0.77 in. in length and weights about 1 oz.

In order to more accurately predict the dynamic behavior of the poppet, a FEM of the part was created by MSFC. MSFC provided their model to GRC so that GRC could use it in our own analysis. The poppet FEM is shown in Figure 5. The model consists of 152,149 elements and 219,182 nodes. The MSC.Nastran element type is CTETRA; a four-sided solid element with four to ten grid points. Several preprocessor checks were used to verify the robustness of the FEM. These checks include free-free edge checks, duplicate grids, element quality, material property units and magnitude, and local coordinate system orientation (Refs. 3 and 4). The model was solved using MSC.Nastran 2008. To further validate the model, several PARAM and analytical diagnostics were performed including MAXRATIO (check for stiffness matrix ill-conditioning), GRDPNT (check of mass properties), GROUNDCHECK (strain energy check), free-free normal modes rigid body modes less than 1×10^{-4}, and finally mode shape evaluation (Refs. 6 and 7).

The next step was to determine the dynamic characteristics of the poppet using the checked-out FEM. Correct definition of the boundary condition is important for a correct modal analysis. The poppet was fixed in translation at every node on the blue surface shown in Figure 5. This mimics the way the actual poppet is constrained in the FCV assembly. Normal modes were solved using MSC.Nastran 2008 solution 103 (Refs. 8 and 9). The resulting natural frequency values are given in Table 3. It should be noted that the first mode given by Nastran was 17,693 Hz. This is only about five percent different from the value computed using hand calculations. This comparison helps to verify the correctness of the FEM. The modal effective mass was also computed and is shown in Table 3. This information indicates what percent of the total mass of the model is moving or rotating in a given direction. The modal results file was imported into NX I–DEAS 5 for mode shape visualization. A select few mode shapes are shown in Table 3. Table 3 shows that there are several poppet modes which lie within the critical frequency range from 94.9 to 128.5 kHz. This is the range, calculated previously, at which a structural acoustic coupling is most likely to occur.

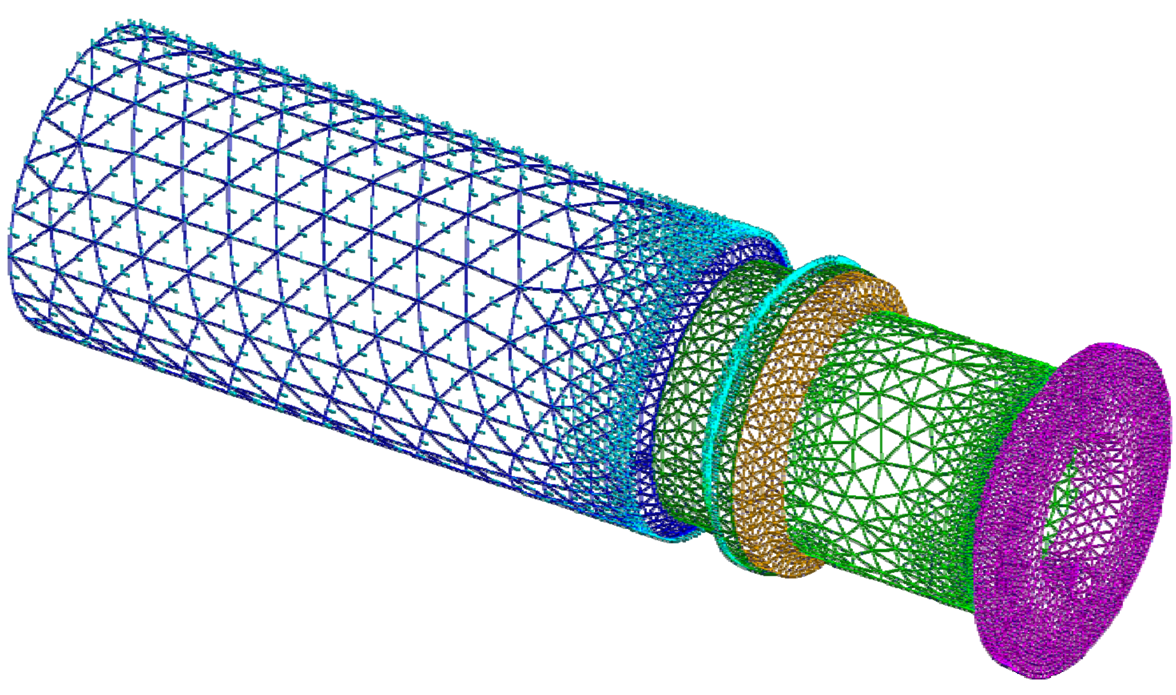

Figure 5.—GH2 FCV Poppet FEM.

TABLE 3.—FCV POPPET NORMAL MODES RESULTS

	MSFC	GRC	% Effective Mass						
#	Hz	Hz	x	y	z	rx	ry	rz	Description of Mode
1	17,693	17,693	0	19	0	0	0	52	Poppet First Bending Y
2	17,694	17,694	0	0	19	0	52	0	Poppet First Bending Z
3	35,868	35,868	0	0	0	23	0	0	Poppet Torsion
4	55,736	55,736	0	8	0	0	0	11	Poppet Second Bending Y
5	55,781	55,781	0	0	8	0	11	0	Poppet Second Bending Z
6	56,191	56,191	28	0	0	0	0	0	Poppet Axial
7	65,154	65,154	0	0	0	0	0	0	Flange Warping (2-axis)
8	65,702	65,702	0	0	0	0	0	0	Off Axis Flange Warping (2-axis)
9	78,027	78,027	0	0	0	0	0	0	Flange Potato Chip
10	78,281	78,281	0	0	0	0	0	0	Flange Potato Chip Off Axis
11	92,474	92,474	0	0	0	5	0	0	Second Poppet Torsional
12	98,077	98,077	0	0	2	0	2	0	Poppet Third Bending Z
13	98,281	98,281	0	2	0	0	0	2	Poppet Third Bending Y
14	109,619	109,619	0	0	0	0	0	0	Flange Second Potato Chip
15	109,728	109,728	0	0	0	0	0	0	Flange Warping Potato Chip
16	114,490	114,490	2	0	0	0	0	0	Poppet Mushroom
17	121,712	121,712	0	0	0	0	0	0	Double Potato Chip
18	121,938	121,938	0	0	0	0	0	0	Double Potato Chip Off Axis
19	123,597	123,597	0	1	0	0	0	1	Poppet Fourth Bending Y
20	124,472	124,472	0	0	1	0	1	0	Poppet Fourth Bending Z
21	141,586	141,586	0	0	1	0	1	0	Poppet Fifth Bending Z
22	142,753	142,753	0	1	0	0	0	1	Poppet Fifth Bending Y
23	146,802	146,802	0	0	0	0	0	0	Flange Potato Chip Bubble
24	147,374	147,374	0	0	0	0	0	0	Off Axis Potato Chip Bubble
25	148,601	148,601	6	0	0	0	0	0	Big Mushroom

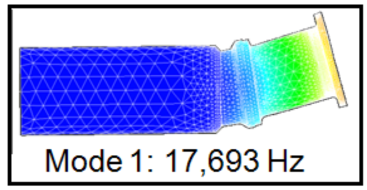

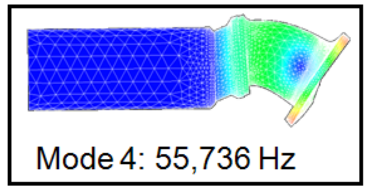

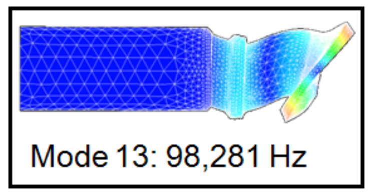

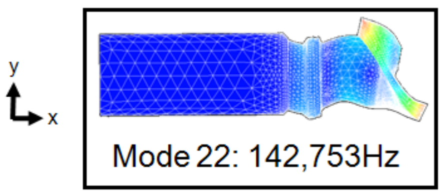

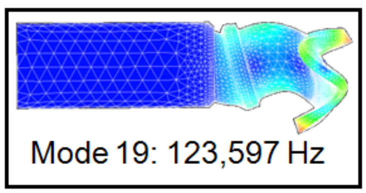

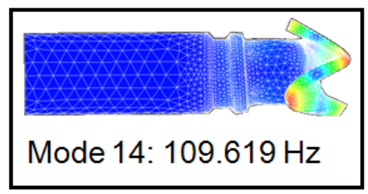

Stress Prediction Methodology

The next step in verifying the structural acoustic coupling is to perform forced and transient response analysis of the FCV. This analysis is performed using the same FEM utilized in determining the structural modes of the poppet. An overview of the stress prediction methodology used is shown in Figure 6. Figure 6 demonstrates the four independent paths taken in determining the cyclic stresses found on the poppet. The input for each of the analysis methods comes from computational fluid dynamics (CFD) results that were provided by MSFC. The CFD result used was the pressure distribution exerted on the poppet as a function of time. Pressures were also provided in the frequency domain as a function of frequency and phase. Two primary methods were used to determine the poppet stresses. The first method is a simpler steady-state method; the second method is a transient method performed in the time domain. Each of the two methods was performed independently by MSFC and GRC using different toolsets. The results are then compared.

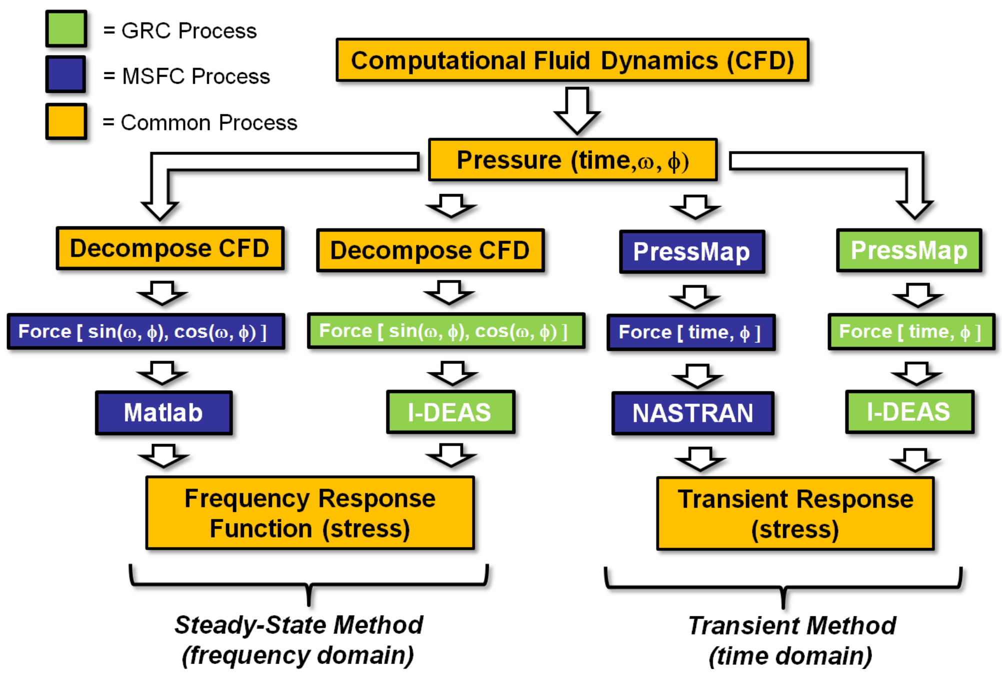

Figure 6.—Stress Prediction Methodology Flowchart.

Steady State Methodology

The first stress prediction method used is a steady-state method performed in the frequency domain (Fig. 6, left half). Figure 7 shows the inputs used in the simulated frequency response analysis. The CFD results were provided as pressures across the poppet face. To simplify the analysis the CFD data is decomposed into a discrete number of resolved forces that contained the appropriate frequency and phase information to approximate the complex pressure distributions given by the CFD model. This resolved forcing function is used as one of the inputs to the frequency response analysis. The resolved forces are applied to the poppet FEM that contains the poppet modal information. Because a flight failure occurred, a conservative value was chosen for damping. 0.25 percent critical damping was used for the analysis. 0.25 percent represents damping inherent to the material only. The result from the frequency response analysis is a stress frequency response function (FRF). The FRF is a plot of stress verses frequency for the highest stress element in each of the three principle directions x, y, and z. MSFC used Matlab to calculate these FRF results. The modal information was taken from the MSC.Nastran output file and combined with the resolved forces in Matlab. GRC used NX I–DEAS 5 to calculate the FRF results. The results were then plotted in Matlab to make an easy comparison with MSFC.

Steady State Results

Results from the steady state simulation are in the form of stress FRF plots. Plotted is the highest stress element for each of the three principle directions. The steady state frequency response analysis was simulated using several different, increasingly complex, forcing functions. Figure 8 shows results for the case in which the CFD data is decomposed into a simple two point forcing function. Also shown on the plots is the location of the 107.4 kHz acoustic mode which was previously determined. Peaks on the plot indicate frequencies where structural modes are being excited by the input forcing function. A peak at around 107.4 kHz would indicate that there is a structural acoustic alignment; Figure 8 shows no such alignment. Figure 8 does indicate that the GRC and MSFC methodologies are both producing very similar results. Any differences in the plots are very minor and considered insignificant. The key information is the same for both analysis methods.

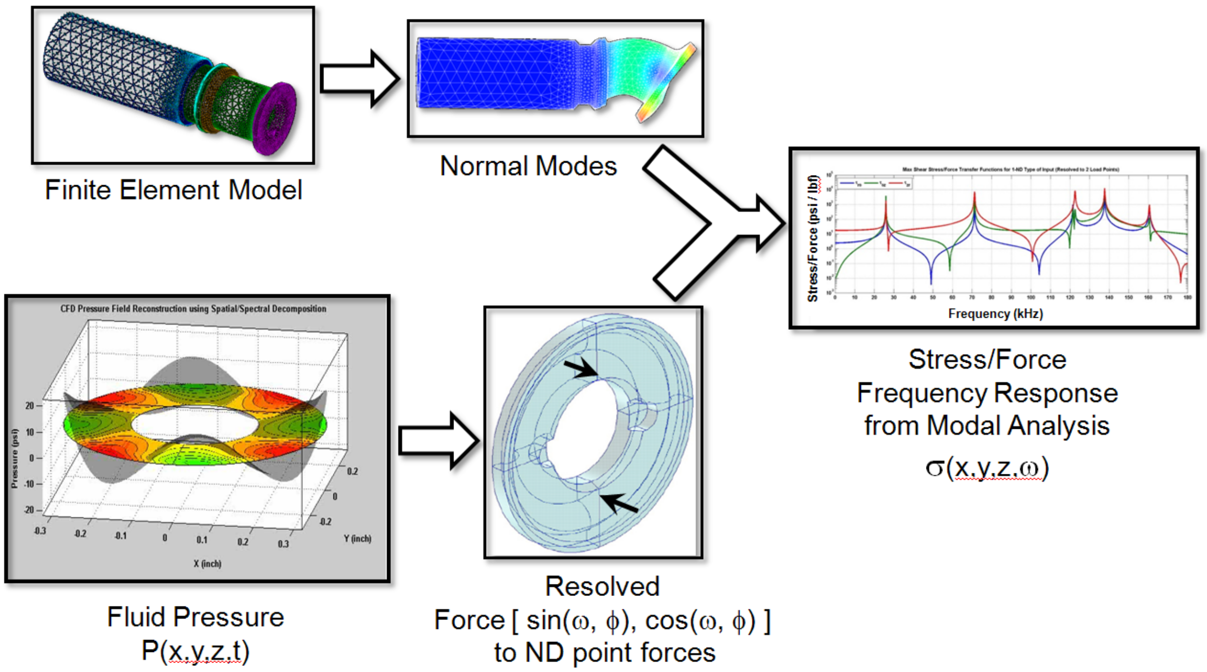

Figure 7.—Steady-State Stress Prediction Methodology.

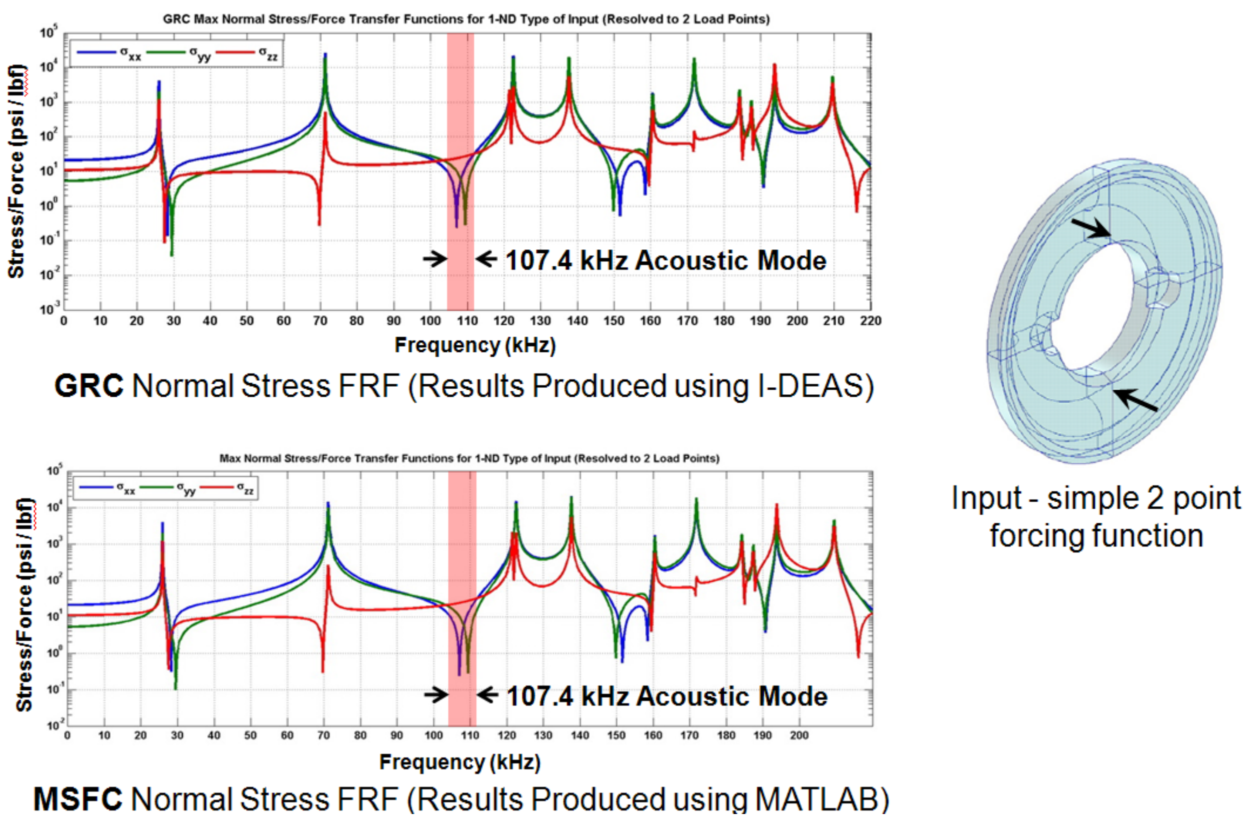

Figure 8.—Steady-State Stress FRF Results for 2-Point Input.

Once the analysis methodology had been developed it is possible to increase the complexity in order to more accurately simulate what was actually occurring. The simple 2-point forcing function input is a fairly crude model of the complex acoustic mode present in the FCV cavity. Figure 9 shows results for the case in which the CFD data has been decomposed into an 8 point forcing function. Once again the 107.4 kHz acoustic mode is shown on the plot. With the increased fidelity input different peaks appear on the plot. This might indicate that the 2-point forcing function was insufficient in accurately representing the input force. Figure 9 shows an obvious peak at 110 kHz, which is nearly perfectly aligned with the 107.4 acoustic mode.

The FRF plots change drastically from the 2-point to the 8-point forcing function. In order to validate the existence of the excited 110 kHz structural mode, the fidelity of the analysis is further increased. The CFD acoustic data is decomposed into a 288-point force applied to the poppet face. The 288-point forces are applied at varied distances in the radial direction on the poppet face in addition to being clocked around the face. Figure 10 shows results for the case where the CFD data has been decomposed into a 288 point forcing function. As with the previous plots, the 107.4 kHz acoustic mode is shown on the plot. Once again there is an obvious peak at 110 kHz. Figures 9 and 10 share several other major peaks indicating that both the 8 and 288 point forcing functions are exciting similar structural modes. This increases confidence that the fidelity of the analysis is sufficient and that the 110 kHz excitation is real.

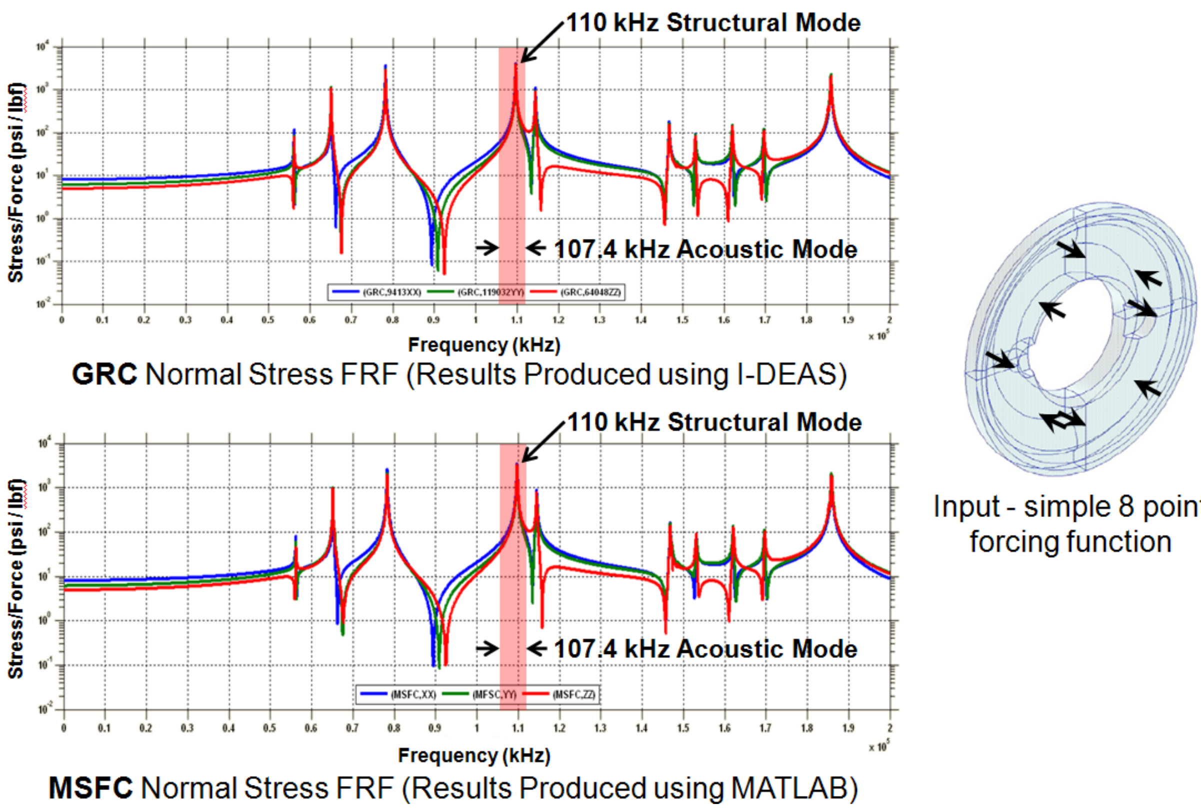

Figure 9.—Steady-State Stress FRF Results for 8-Point Input.

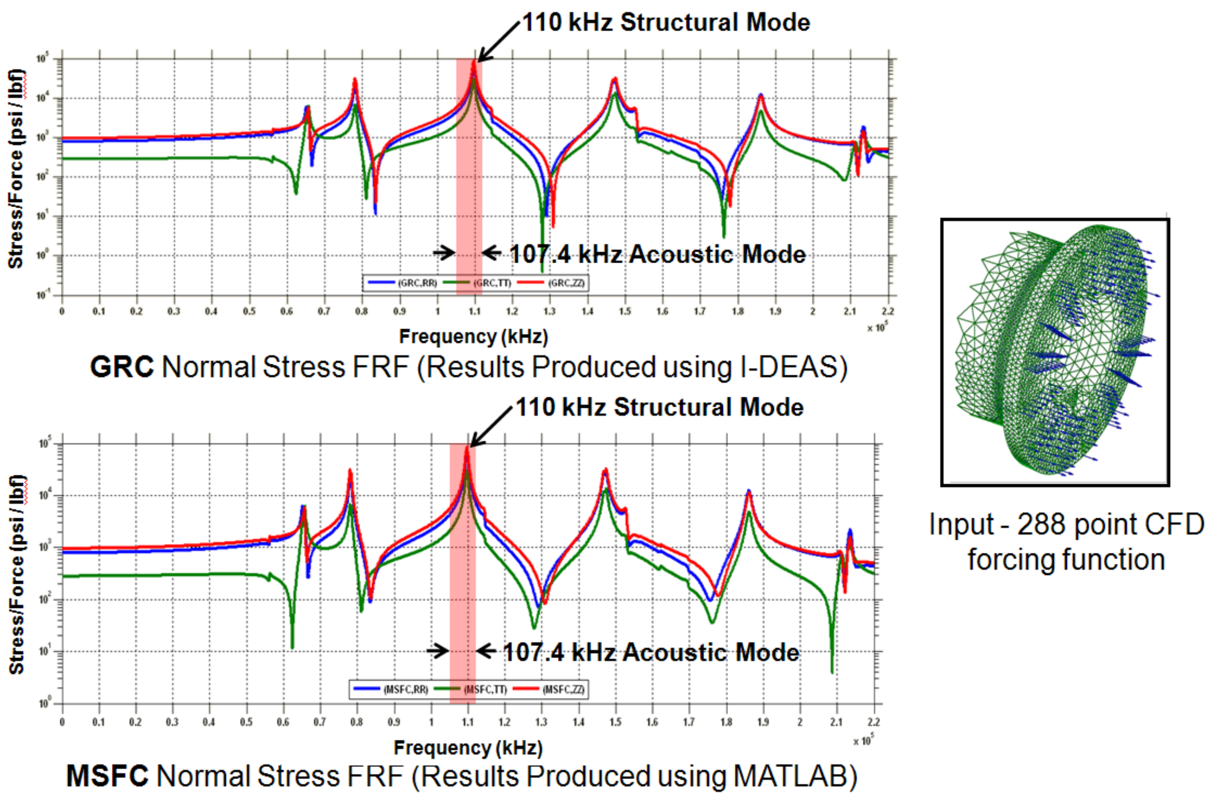

Figure 10.—Steady-State Stress FRF Results for 288-Point Input.

Transient Methodology

The steady-state method is performed in the frequency domain. The second method used is a transient method carried out in the time domain (Fig. 6, right half). Figure 11 shows the inputs used in the transient response simulation. The CFD results are provided as pressures across the poppet face. The software PressMap is used to remap the CFD results onto the nodes of the FEM since the CFC and FEM meshes are dissimilar. The result of this mapping is a unique input force, which varies as a function of time, applied to every node on the poppet face. The time varying forces are then applied to the FEM to produce transient response results. These results plot stress verses time for the four highest stressed elements. The values of stress being plotted are the maximum principal stresses. MSFC used PressMap to remap the pressures and MSC.Nastran to perform the transient simulation. GRC used PressMap to solve for the remapped pressures and then NX I–DEAS 5 to run the transient simulation. The results from both parties are plotted in Matlab for comparison purposes.

Transient Results

Results from the transient analysis are in the form of stress verses time plots. Plotted is the maximum principal stress for the four highest stressed elements. These elements are typically located in the poppet flange fillet. Figure 12 shows the stress state in the poppet for 0.15 msec of acoustic loading. Figure 12 shows both results computed by GRC using NX I–DEAS 5 and MSFC using MSC.Nastran. There are slight differences in the plots which can perhaps be attributed to the different solution codes used during the solve. The overall trends of the two plots are the same. Both plots show a cyclic stress state in the poppet flange fillet that increases in amplitude. The plot has 11 distinct peaks over the last 0.1 msec of acoustic loading; this equates to a 110 kHz stress oscillation frequency.

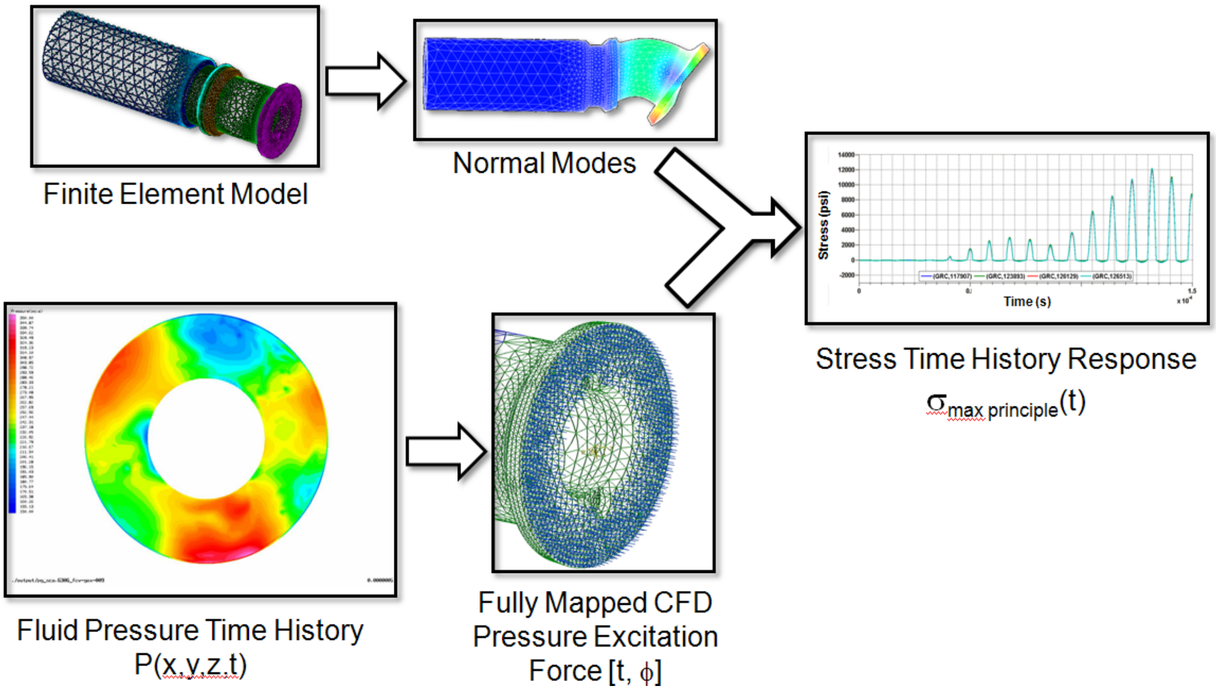

Figure 11.—Transient Stress Prediction Methodology.

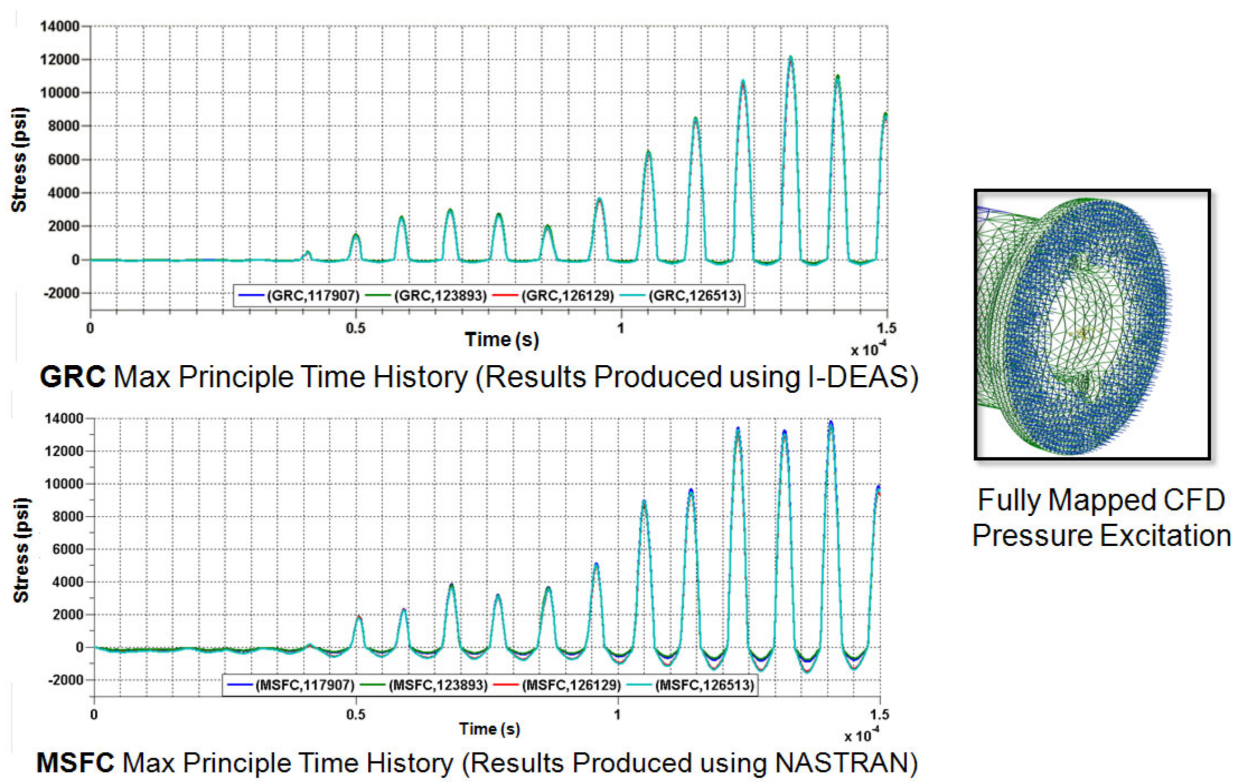

Figure 12.—Transient Stress Results.

Conclusions

The critical frequency calculation indicates that there is structural acoustic coupling from approximately 94.9 to 128.5 kHz. Both the acoustic and structural dynamic analyses indicate that there is a critical acoustic mode at 107.4 kHz that aligns with a structural mode at 110 kHz. During this coupling a relatively high stress state occurs in the poppet fracture region. Due to the coupling, high cycle fatigue is thought to be initiated during the high flow condition. This high cycle fatigue could initiate cracks in the poppet. During the low flow condition a high static pressure is applied to the poppet flange. This high static pressure could lead to further crack growth and eventual failure. As a result of this analysis establishing the structural acoustic coupling, NASA is proceeding to mitigate the risk by performing post flight FCV poppet inspections for all remaining flights. Additionally, GH2 FCVs are to be removed after every flight and refurbished.

References

1. Unknown, "STS–119 Flight Readiness Review," Space Shuttle Program, Orbiter & GFE Project, Feb. 3, 2009.
2. Unknown, "STS–119 Flight Readiness Review," Space Shuttle Program, Orbiter & GFE Project, Feb. 20, 2009.
3. Unknown, "MPS GH2 Flow Control Valve Poppet Failure Investigation Summary," PRCB, Jan. 7, 2010
4. L.L. Beranek, "Noise and Vibration Control," Chapter 11, 1971.
5. R.D. Blevins, "Formulas For Natural Frequency And Mode Shape," Krieger Publishing Company Malabar, FL, 1993.
6. "Practical Dynamic Analysis in MSC/NASTRAN," NASA 116, Section 2, 2004.
7. T.P. Serafin, "Spacecraft Structures and Mechanisms: From Concept to Launch," pp. 592–593, 2003.
8. MSC Software Corporation, "MSC.Nastran 2005 Quick Reference Guide," 2005.
9. MSC Software Corporation, "NAS102—MSC.Nastran Dynamic Analysis Exercises Vol. 1", Santa Ana, CA, 2004.

REPORT DOCUMENTATION PAGE					*Form Approved* *OMB No. 0704-0188*

1. REPORT DATE *(DD-MM-YYYY)* 01-05-2010	**2. REPORT TYPE** Technical Memorandum	**3. DATES COVERED** *(From - To)*
4. TITLE AND SUBTITLE Analysis of the STS-126 Flow Control Valve Structural-Acoustic Coupling Failure		**5a. CONTRACT NUMBER**
		5b. GRANT NUMBER
		5c. PROGRAM ELEMENT NUMBER
6. AUTHOR(S) Jones, Trevor, M.; Larko, Jeffrey, M.; McNelis, Mark, E.		**5d. PROJECT NUMBER**
		5e. TASK NUMBER
		5f. WORK UNIT NUMBER WBS 377816.06.02.02.03
7. PERFORMING ORGANIZATION NAME(S) AND ADDRESS(ES) National Aeronautics and Space Administration John H. Glenn Research Center at Lewis Field Cleveland, Ohio 44135-3191		**8. PERFORMING ORGANIZATION REPORT NUMBER** E-17276
9. SPONSORING/MONITORING AGENCY NAME(S) AND ADDRESS(ES) National Aeronautics and Space Administration Washington, DC 20546-0001		**10. SPONSORING/MONITOR'S ACRONYM(S)** NASA
		11. SPONSORING/MONITORING REPORT NUMBER NASA/TM-2010-216339

12. DISTRIBUTION/AVAILABILITY STATEMENT
Unclassified-Unlimited
Subject Categories: 16 and 20
Available electronically at http://gltrs.grc.nasa.gov
This publication is available from the NASA Center for AeroSpace Information, 443-757-5802

13. SUPPLEMENTARY NOTES

14. ABSTRACT
During the Space Transportation System mission STS-126, one of the main engine's flow control valves incurred an unexpected failure. A section of the valve broke off during liftoff. It is theorized that an acoustic mode of the flowing fuel, coupled with a structural mode of the valve, causing a high cycle fatigue failure. This report documents the analysis efforts conducted in an attempt to verify this theory. Hand calculations, computational fluid dynamics, and finite element methods are all implemented and analyses are performed using steady-state methods in addition to transient analysis methods. The conclusion of the analyses is that there is a critical acoustic mode that aligns with a structural mode of the valve.

15. SUBJECT TERMS
Dynamics; Dynamic structural analysis; Dynamic response; Acoustics; Control valves; Space shuttles; Spacecraft models; Dynamic models; Acoustic coupling

16. SECURITY CLASSIFICATION OF:			**17. LIMITATION OF ABSTRACT**	**18. NUMBER OF PAGES**	**19a. NAME OF RESPONSIBLE PERSON** STI Help Desk (email:help@sti.nasa.gov)
a. REPORT U	**b. ABSTRACT** U	**c. THIS PAGE** U	UU	20	**19b. TELEPHONE NUMBER** *(include area code)* 443-757-5802